Efficient Control strategy based on instantaneous power theory and model predictive control for grid connected photovoltaic system

Ricsa Alhassane Soumana[1], Michael Juma Saulo[2], Christopher Maina Muriithi[3].
[1]Pan African University Institute for Basic Sciences, Technology and Innovation, Nairobi, Kenya,
[2]Technical University of Mombasa, Mombasa, Kenya
[3]Murangá University of Technology, Murangá, Kenya

Abstract

Due to the rapid decline of fossil resources and the impact of their use for electric power generation on the environment, renewable energy sources are increasingly explored and integrated into the power grid. Among the Renewable energy sources, photovoltaic (PV) systems are one of the most integrated into the utility grid. Thus, this paper presents a control scheme based on instantaneous power theory (IPT)and model predictive control (MPC) to inject the PV power into the grid at unity power factor with minimum current harmonics. The proposed control strategy is applied to a two-stage grid connected PV system which employs boost converter and two-level voltage source inverter. The current references are obtained in the dq reference frame based on IPT. A finite control set model predictive control (FCS-MPC) is used to control the inverter current in order to inject with high accuracy the current references into the grid. The effectiveness and the performance of the proposed control strategy is confirmed by MATLAB/Simulink under various solar irradiance level.

Keywords: Grid Connected PV System, Instantaneous Power Theory, Model Predictive Control, THD.

1. Introduction

Global energy crisis and environmental concerns from exhaustible fossil fuels have pushed numerous researchers to alternative energy sources which are inexhaustible and produce less environmental impact(M. vinary Kumar, 2020). Among various alternative energy sources, the solar energy has a cutting edge over others(Patil, n.d.). Grid connected photovoltaic system (GCPVS), compared to off-grid system, has advantage of not requiring storage system. The integration of PV energy production into grid is experiencing a significant growth in recent years. Since the Penetration of the Solar PV energy has been increased rapidly over the decade, the issue of maintaining the power quality within the allowable range has been a topic of major concern(Obi & Bass, 2016). The widespread integration of inverters for integrating distributed units with the grid has lead harmonics distortion and complications in attaining frequency stability(Liang, 2017). The power quality at the point of common coupling(PCC) is an important parameters to the utilization of PV energy(Reveles-Miranda et al., 2020). In GCPVS, one of the major power quality concerns is the harmonics and the total harmonic distortion (THD) is the most useful way to assess harmonics of a given signal.

The performance of GCPVS depends mainly on the control scheme applied(Zeb et al., 2018) and the control of the inverter is one of the most significant part of the GCPVS (Arulkumar et al., 2016; Zeb et al., 2018). The grid connected inverters require a suitable control technique in order to inject pure sinusoidal current into the grid(Sinha et al., 2018). In this sense that several controllers of PV inverters including Proportional-Integral(P-I) controllers (Liu et al., 2014; Selvaraj & Rahim, 2009), proportional resonant controllers (Tariq et al., 2017; Ye et al., 2016), linear quadratic regulators (Huerta et al., 2012; Xie et al., 2020), sliding mode controllers (Benadli et al., 2015), neural network controllers (Kalla, 2017; Kaushik et al., 2020), fuzzy logic controllers (Hannan et al., 2014; Ramalingeswara Rao & Srikanth, 2014), repetitive controllers(Gao et al., 2018), hysteresis controllers (Mosazadeh et al., 2012; Rahim et al., 2007) , predictive controllers (Ahmed et al., 2020; Boukezata et al., 2016; Long et al., 2021) have been developed in order to inject high current quality into the grid. The classical PI controllers can not eliminate the steady state error (Arulkumar et al., 2016). The proportional resonant controllers cannot achieve the fully power factor control in the αβ coordinates control strategy and they become more complex in the abc reference frame control strategy (Arulkumar et al., 2016). The current regulation by hysteresis regulator is highly complex (Arulkumar et al., 2016; Sinha et al., 2018) and present variable switching frequency(Arulkumar et al., 2016). for neural network controller, to find the proper learning is though(Babu P et al., 2020). Sliding mode controllers suffer from chattering effect which in certain can even damage the actuator (Zhu & Fei, 2017). Fuzzy logic controllers must be carefully tuned to achieve maximum performance(Justin Boitano, n.d.) and the choice of fuzzy membership function as well as scaling gain may be a tedious process.

Due to the rapid improvement in the microprocessor, the mathematical control techniques such as MPC become an effective method to control several applications with different control variables (Abdelrahem et al., 2020). The subset known as finite-control set model predictive control(FCS-MPC) is the most intuitive implementation of MPC, as control actions are considered directly, and eliminates the need of a modulator(Easley et al., 2021). Several varieties of control scheme based on FCS-MPC have been proposed in the literature such as FCS-MPC with Kalman filtering capability (Ahmed et al., 2020), Synchronous Reference Frame Theory based on FCS-MPC(Sathiyanarayanan & Mishra, 2016), A Lyapunov function based model predictive control (Golzari et al., 2019) to enhance the THD level of the injected current into the grid .

In this paper, a control scheme based on IPT and FCS-MPC is proposed to inject the PV power into the grid at unity power factor with minimum current THD. The main advantages of the proposed control scheme are its simplicity and its effectiveness under various solar irradiance level. The rest of the paper is structured as follows: Section 2 presents the description of the studied system. Section 3 describes the proposed control strategy. The simulation results are presented and discussed in section 4. Finally, concluding remarks are given in section 5.

2. Description of the studied system

The schematic diagram of the studied grid connected photovoltaic system is shown in Figure 1. The studied system has three phase utility grid which is connected to a PV array. The latter is integrated into the grid via a boost converter and two-level voltage source inverter. a direct duty cycle control P&O maximum power point tracking (MPPT) method(Pandiarajan et al., 2012) which is the most used in practice is applied to the dc boost converter to extract the maximum available power of the PV array. A PI controller is employed to keep the dc bus voltage at its reference. The θ represent the grid phase angle information obtained by Phase Lock Loop (PLL).

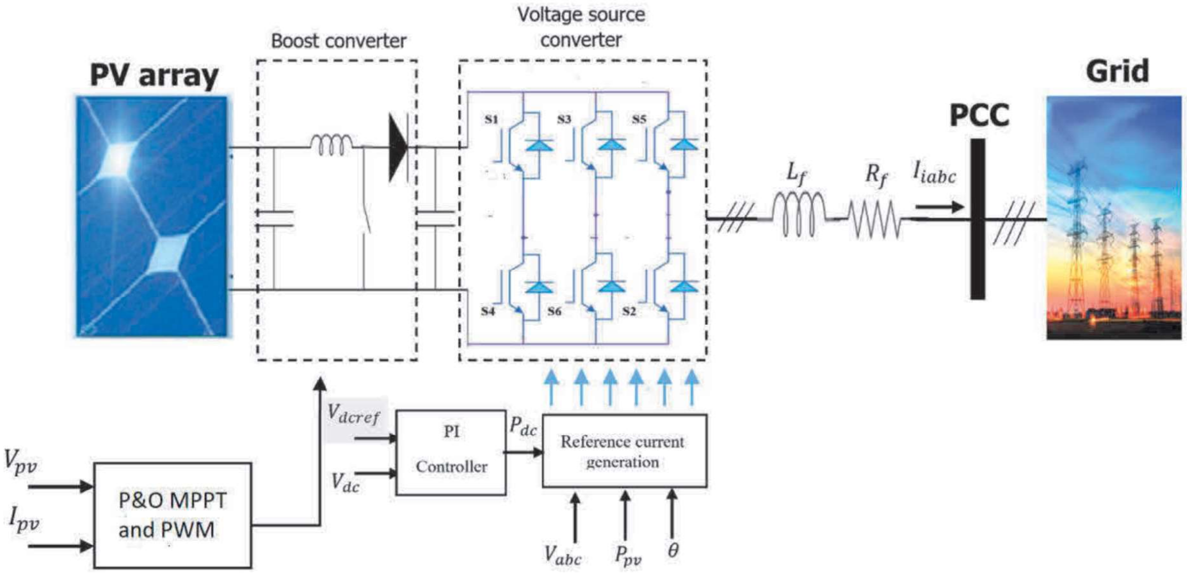

Figure 1: Structure of the Studied System

2.1 PV array modeling

In this paper, a single diode model which is the most commonly employed(Mohamed Rida et al., 2018) is used and its PV cell equivalent circuit is shown in Figure 2(Villalva et al., 2009). The current(I_{pv})-voltage (V_{pv}) relationship is given by(Villalva et al., 2009):

$$I_{pv} = I_{ph} - I_d - I_{sh} \quad (1)$$

$$I_{pv} = I_{ph} - I_s\left[\exp\left(\frac{V_{pv} + R_S I_{pv}}{AV_t} - 1\right)\right] - \left(\frac{V_{pv} + R_S I_{pv}}{R_{sh}}\right) \quad (2)$$

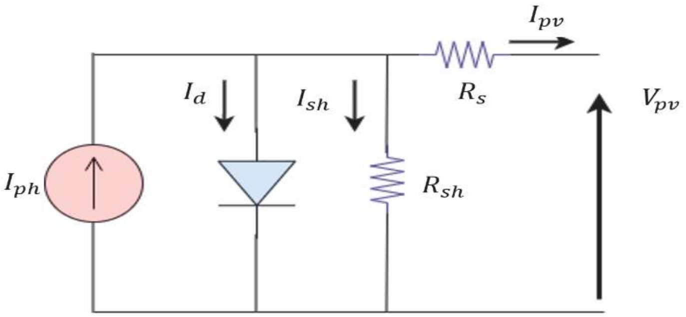

Figure 2: Equivalent Circuit of a PV cell

Where R_s and R_{sh} are respectively the equivalent series and parallel resistance of the PV cell. I_{ph} and I_s represent the current generated by the incident light and saturation currents of the diode. Their equations are well described in reference (Villalva et al., 2009). $V_t = \frac{N_s KT}{q}$ is the thermal voltage of the PV cell with N_s cells connected in series. K is the Boltzmann constant ($K = 1.38 \times 10 - 23$ J/K), q is the electron charge ($q = 1.6 \times 10 - 19$ C), T is the absolute temperature in Kelvin, and A is the diode ideality factor.

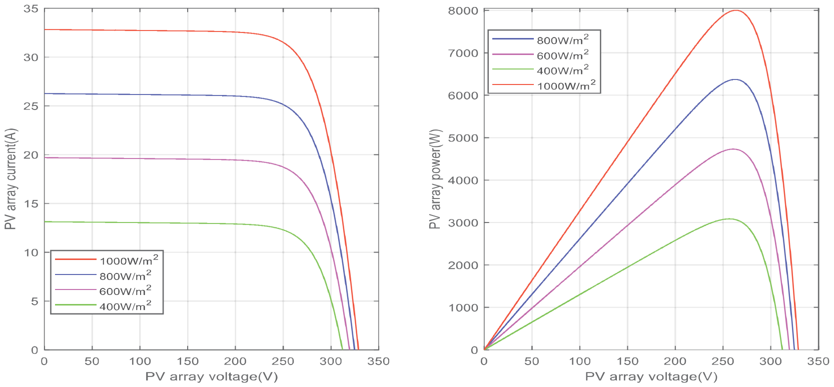

(a) (b)

Figure 3: (a) $I_{pv} - V_{pv}$ Characteristics; (b) $P_{pv} - V_{pv}$ Characteristic

The Kyocera KC200GT PV module is used to make a PV generator of 8KWp. The PV generator consist of 10 modules in series and 4 modules in parallel. The $I_{pv}(V_{pv})$ and $P_{pv}(V_{pv})$ characteristics of the PV generator at fixed temperature (25^0C) and different solar irradiance level are shown in Figure 3.

3. IPT-based FCS-MPC

In three phase system, active and reactive power is suitably controlled by using the approach of dq rotating synchronous frame (Arulkumar et al., 2016). According to the IPT, the active power P and reactive power Q under dq synchronous rotating reference frame can be expressed as follows(Huang et al., 2013):

$$P = \frac{3}{2}\left(v_d i_d + v_q i_q\right) \tag{3}$$

$$Q = \frac{3}{2}\left(v_q i_d - v_d i_q\right) \tag{4}$$

If the rotating frame is aligned with the A-axis of the grid voltage vectors, The d-axis and q-axis references current can be expressed as :

$$i_{d\_ref} = \frac{2P_{ref}}{3v_d} \tag{5}$$

$$i_{q\_ref} = \frac{-2Q_{ref}}{3v_d} \tag{6}$$

The reference active power (P_{ref}) to be injected into the grid is obtained by subtracting the output of the PI controller (P_{dc}) from the power generated by the PV array (P_{pv}) (Lalouni & Rekioua, 2013). The reference reactive power to be injected is given by an external command and it is held at zero in this paper.

$$P_{ref} = P_{pv} - P_{dc} \tag{7}$$

Equation (5) and (6) are transformed in the αβ reference frame to get the references current for the MPC controller. The prediction of the injected current(Boukezata et al., 2016) and cost function(Almaktoof, 2014; Boukezata et al., 2016)in the α-β coordinates are respectively given by equation (8) and (9)

$$i_{i\alpha\beta}{}^{p}(k+1) = \left(1 - \frac{R_f T_s}{L_f}\right) i_{i\alpha\beta}(k) + \frac{T_s}{L_f}\left[v_{i\alpha\beta}(k) - v_{\alpha\beta}(k)\right] \tag{8}$$

$$g = \left(i_{i\alpha}^{*}(k) - i_{i\alpha}^{p}(k+1)\right) + \left(i_{i\beta}^{*}(k) - i_{i\beta}^{p}(k+1)\right) \tag{9}$$

$v_{i\alpha\beta}$ and $v_{\alpha\beta}$ are respectively the voltage generated at the output of the inverter and grid voltages in the αβ coordinates. T_s is the sampling period. For a two-level voltage source inverter, 8 switching states are generated which produce 7 different voltage vectors. For each voltage vector, equation (8) is used to predict the future injected current and equation (9) is used to minimize the error between the reference current and the predicted one. The overall control scheme is depicted in Figure (4)

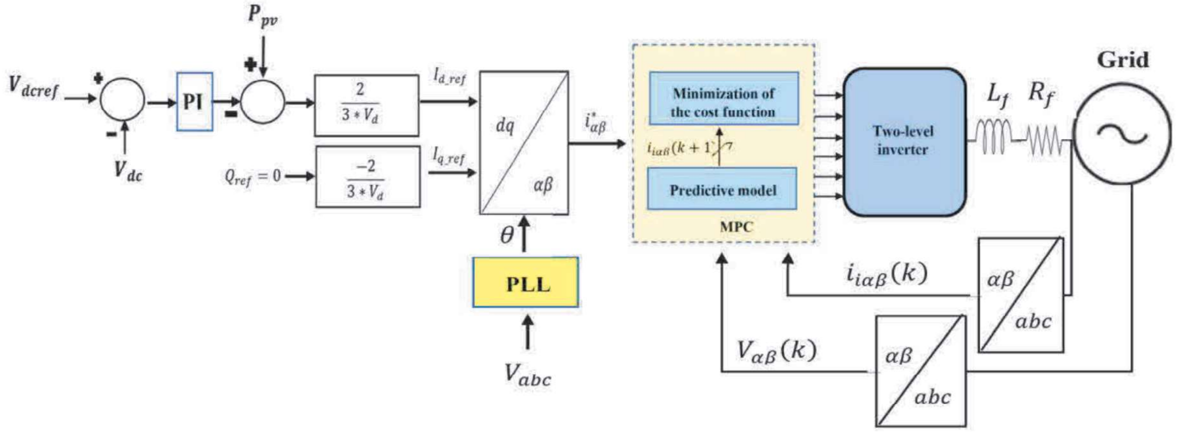

Figure 4: IPT Based FSC-MPC

4. Simulation results and discussion

The proposed control strategy is simulated under various Irradiance level. The system specifications are given in Table 1. Isc and Voc are respectively the short circuit current and open circuit voltage of one PV module. The subscript mpp stand for maximum power point. The system is simulated under different level solar irradiance and current THD is monitored at each solar irradiance level.

Figure 5 present the simulation results when a solar irradiance (G) of 1000W/m^2 is applied from time $t = 0s$ to $t = 0.25s$, then the solar irradiance falls to 800W/m^2 at $t = 0.25s$. during the interval where G = 1000W/m^2 , the injected power oscillates around it reference with an amplitude of around ±22W. from t = 25s, the PV power falls to 6372W and consequently the reference power drops from 7783W to 6175W. in this time interval, the injected power oscillates between 6180W and 6185W.

Table 1: System Specifications

Parameters	Values
Grid voltage	220V
Frequency	50Hz
Capacitors	2200µF
Boost inductor and switching frequency	1.6mH, 5KHz
Coupling inductor (L_f,R_f) ; T_s	2.2mH, 0.01Ω ; 1µs
PI regulator, P_{mpp}, V_{mpp}, I_{mpp}, I_{sc} and V_{oc}	Kp=218; ki=10 ; 200.143W, 26.3V, 7.61A, 8.21A, 32.9V

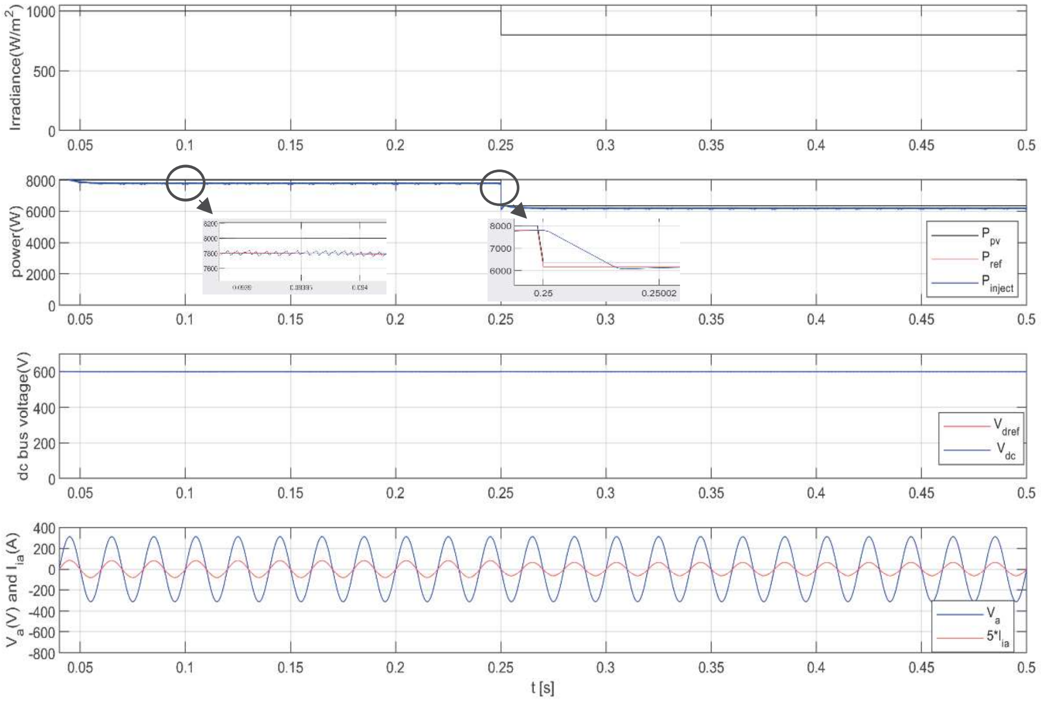

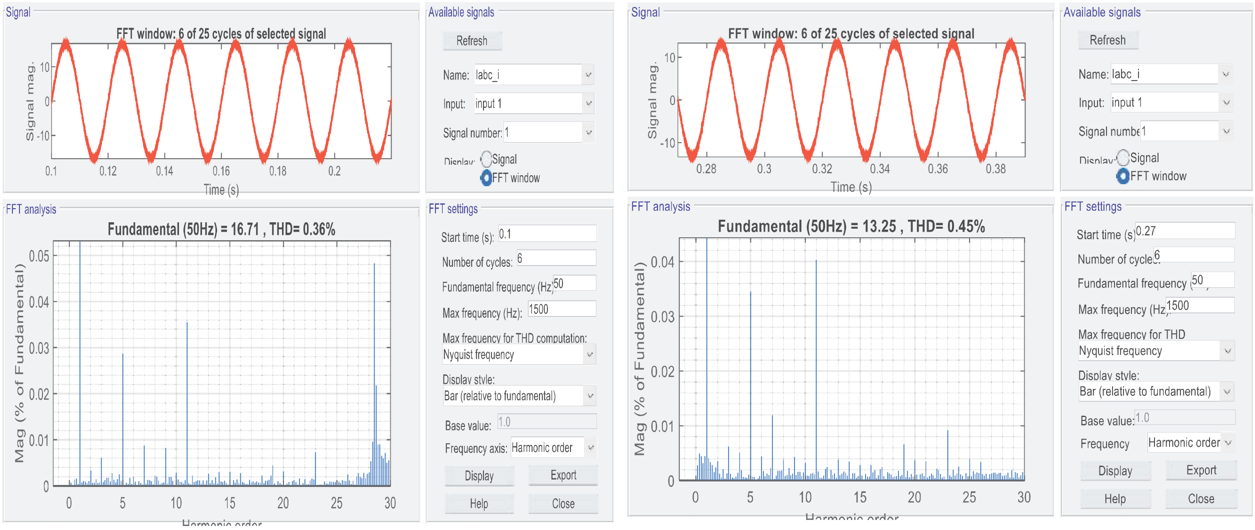

FFT window: 6 of 25 cycles of selected signal

Name: Iabc_i
Input: input 1
Signal number: 1
Display: ○ Signal ● FFT window

Fundamental (50Hz) = 16.71 , THD= 0.36%

Start time (s): 0.1
Number of cycles: 6
Fundamental frequency (Hz): 50
Max frequency (Hz): 1500
Max frequency for THD computation: Nyquist frequency
Display style: Bar (relative to fundamental)
Base value: 1.0
Frequency axis: Harmonic order

FFT window: 6 of 25 cycles of selected signal

Name: Iabc_i
Input: input 1
Signal number: 1
Display: ○ Signal ● FFT window

Fundamental (50Hz) = 13.25 , THD= 0.45%

Start time (s): 0.27
Number of cycles: 6
Fundamental frequency (Hz): 50
Max frequency (Hz): 1500
Max frequency for THD: Nyquist frequency
Display style: Bar (relative to fundamental)
Base value: 1.0
Frequency: Harmonic order

Figure 5: simulation results for a solar irradiation variation from 1000W/m2 to 800W/m2

The simulation results for a G = 600W/m^2 and 400W/m^2 are depicted in Figure 6. Once more the solar irradiance variation has occurred at t = 0.25s. From that time, the injected power into the grid has dropped from 4575W to 4520W. the injected power tracks it references with minimum oscillations.

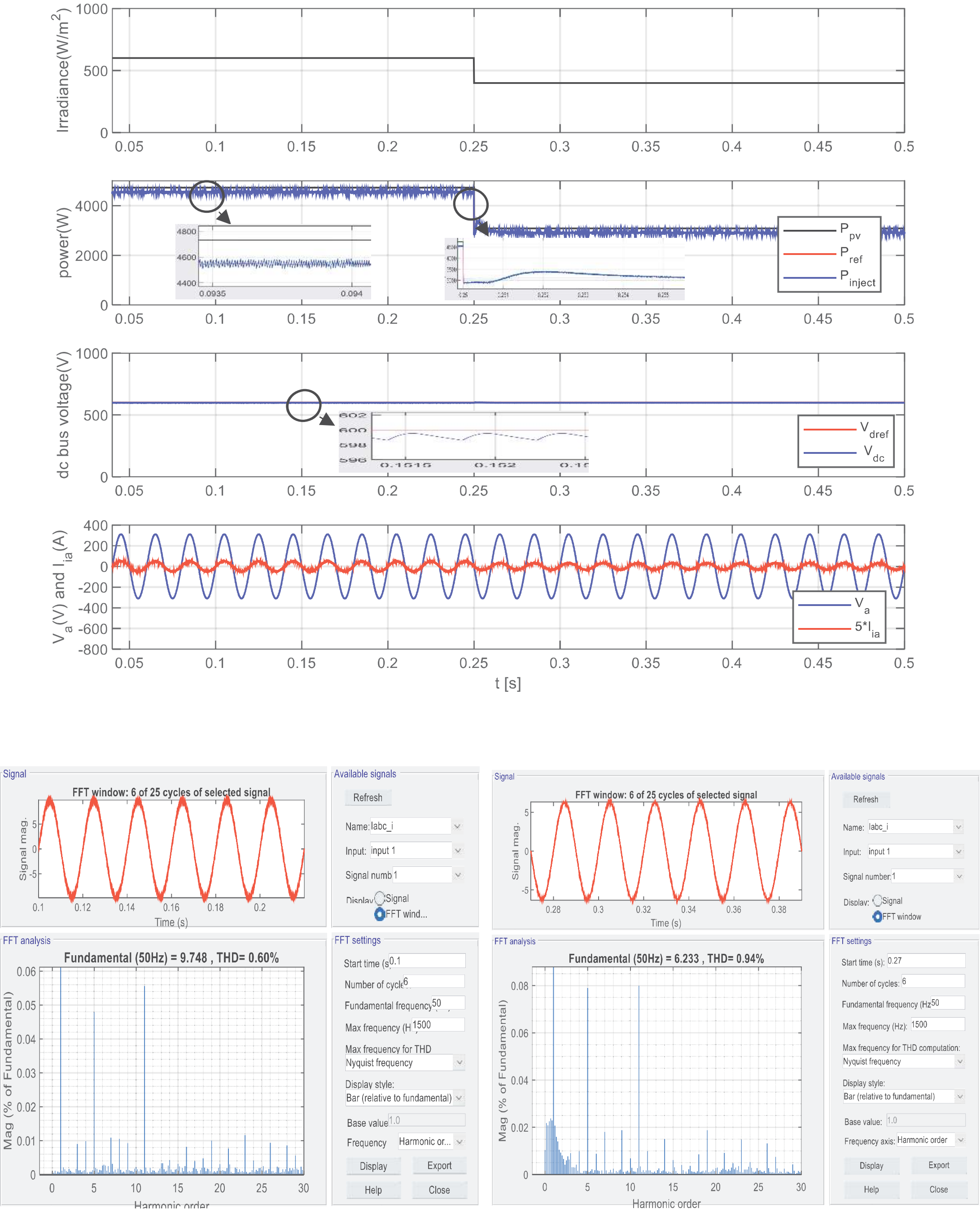

Fundamental (50Hz) = 9.748 , THD= 0.60%

Name: labc_i
Input: input 1
Signal numb 1
Display: ○ Signal ● FFT wind...
Start time (s) 0.1
Number of cycle 6
Fundamental frequency 50
Max frequency (H 1500
Max frequency for THD: Nyquist frequency
Display style: Bar (relative to fundamental)
Base value 1.0
Frequency Harmonic or...

Fundamental (50Hz) = 6.233 , THD= 0.94%

Name: labc_i
Input: input 1
Signal number: 1
Display: ○ Signal ● FFT window
Start time (s): 0.27
Number of cycles: 6
Fundamental frequency (Hz 50
Max frequency (Hz): 1500
Max frequency for THD computation: Nyquist frequency
Display style: Bar (relative to fundamental)
Base value: 1.0
Frequency axis: Harmonic order

Figure 6: Simulation results for a solar irradiation variation from 600W/m^2 to 400W/m^2

Finally a simulation is made for a variation of G from 900W/m^2 to 200WW/m^2 and the simulation results are presented in Figure 7. The voltage at the PCC is imposed by the grid, therefore the injected current is the image of the transferred power. The injected current has suddenly dropped from 15A to 2.8A due to the important decrease in solar irradiance level.

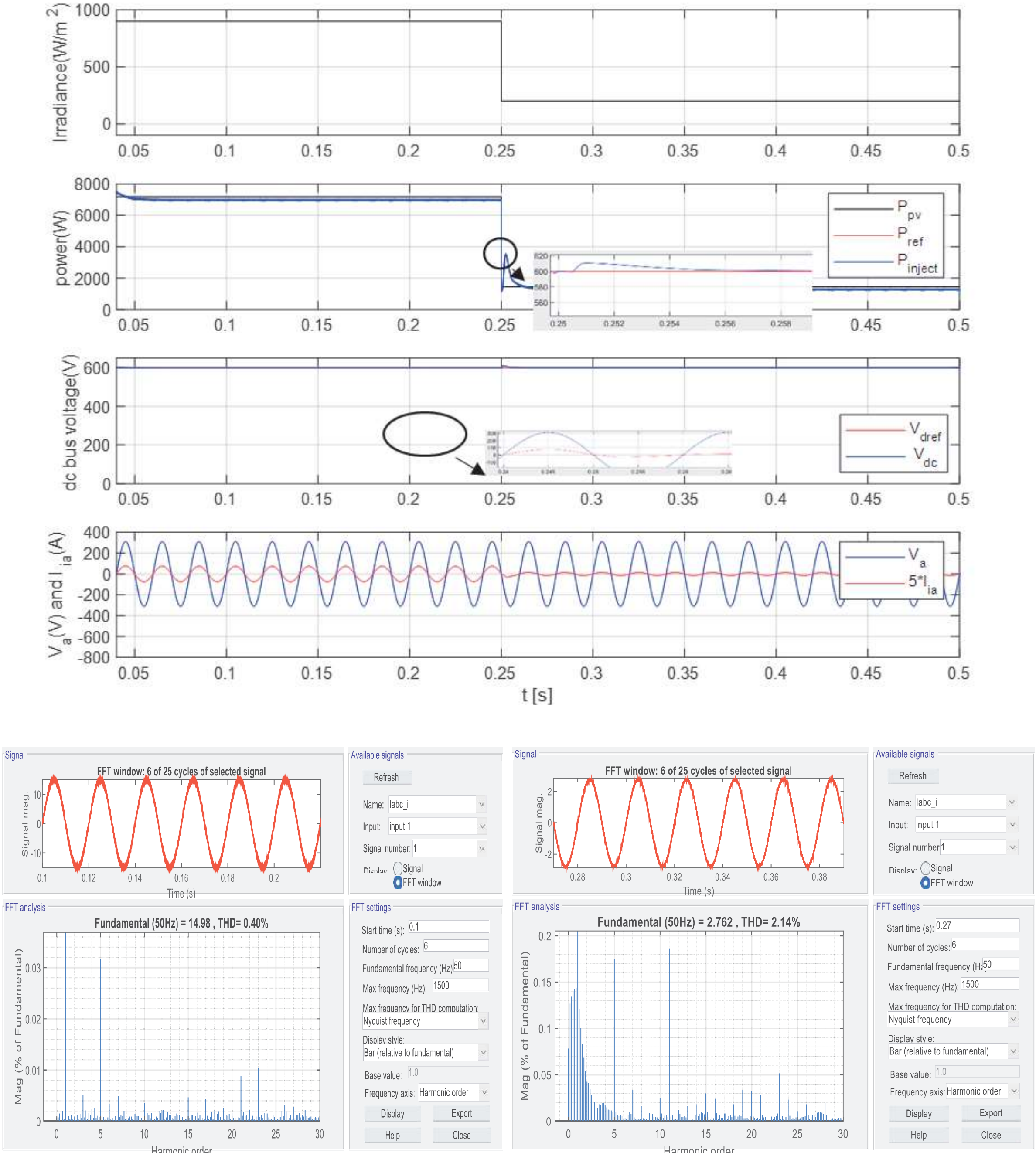

FFT window: 6 of 25 cycles of selected signal

Name: labc_i
Input: input 1
Signal number: 1
Display: ○ Signal ● FFT window

Fundamental (50Hz) = 14.98 , THD= 0.40%

FFT settings
Start time (s): 0.1
Number of cycles: 6
Fundamental frequency (Hz): 50
Max frequency (Hz): 1500
Max frequency for THD computation: Nyquist frequency
Display style: Bar (relative to fundamental)
Base value: 1.0
Frequency axis: Harmonic order

FFT window: 6 of 25 cycles of selected signal

Name: labc_i
Input: input 1
Signal number 1
Display: ○ Signal ● FFT window

Fundamental (50Hz) = 2.762 , THD= 2.14%

FFT settings
Start time (s): 0.27
Number of cycles: 6
Fundamental frequency (Hz): 50
Max frequency (Hz): 1500
Max frequency for THD computation: Nyquist frequency
Display style: Bar (relative to fundamental)
Base value: 1.0
Frequency axis: Harmonic order

Figure 7: Simulation results for a solar irradiation variation from 900W/m^2 to 200W/m^2

In all the simulation results, there is difference between the maximum PV power extracted by the MPPT algorithm and the reference power. This is especially due to the equation (7) in the control process. The variation of solar irradiance has an impact on the current THD

(Patsalides et al., 2007), which can also be noticed from the simulation results. The current THD for all the operating point are given in Table 2. The higher the solar irradiance level, the lesser the injected current THD. All the studied operating point exhibit a grid current THD level lower than the 5% of the IEEE standard 519-19992. Moreover, for all the solar irradiance level simulated, the dc bus voltage is kept at it reference (600V) with no more than 1.5% ripples.

Table 2: Current THD for different of solar irradiance

G(W/m^2)	The injected current THD (%)
1000	0.36
900	0.4
800	0.45
600	0.6
400	0.94
200	2.14

5. Conclusion

In this paper, instantaneous power theory based on model predictive control is proposed to efficiently control a grid connected photovoltaic system. the simulation results confirm the performances of the proposed method in terms of current THD injected into the grid even under low irradiance level. A practical implementation is recommended for a future work.

References

Abdelrahem, M., Ismeil, M. A., Ali, A., Gaafar, M. A., & Kennel, R. (2020). Weight optimisation for model predictive control based on particle swarm optimisation. *PCIM Europe Conference Proceedings*, *1*(July), 1418–1424.

Ahmed, M., Abdelrahem, M., & Kennel, R. (2020). Highly efficient and robust grid connected photovoltaic system based model predictive control with Kalman filtering capability. *Sustainability (Switzerland)*, *12*(11). https://doi.org/10.3390/su12114542

Almaktoof, A. (2014). Modeling and Simulation of Three-Phase Voltage Source Inverter Using a Model Predictive Current Control. *International Journal of Innovation, Management and Technology*, *5*(1), 9–13. https://doi.org/10.7763/ijimt.2014.v5.477

Arulkumar, K., Palanisamy, K., & Vijayakumar, D. (2016). Recent advances and control techniques in grid connected Pv system - A review. *International Journal of Renewable Energy Research*, *6*(3), 1037–1049.

Babu P, N., Guerrero, J. M., Siano, P., Peesapati, R., & Panda, G. (2020). An Improved Adaptive Control Strategy in Grid-Tied PV System With Active Power Filter for Power Quality Enhancement. *IEEE Systems Journal*, *15*(2), 2859–2870. https://doi.org/10.1109/JSYST.2020.2985164

Benadli, R., Khiari, B., & Sellami, A. (2015). Three-phase grid-connected photovoltaic system with maximum power point tracking technique based on voltage-oriented control and using sliding mode controller. *2015 6th International Renewable Energy Congress, IREC 2015*, 0–5. https://doi.org/10.1109/IREC.2015.7110963

Boukezata, B., Gaubert, J. P., Chaoui, A., & Hachemi, M. (2016). Predictive current control in multifunctional grid connected inverter interfaced by PV system. *Solar Energy*, *139*, 130–141. https://doi.org/10.1016/j.solener.2016.09.029

Easley, M., Shadmand, M. B., & Abu-Rub, H. (2021). Hierarchical Model Predictive Control of Grid-Connected Cascaded Multilevel Inverter. *IEEE Journal of Emerging and Selected Topics in Power Electronics*, *9*(3), 3137–3149. https://doi.org/10.1109/JESTPE.2020.3015128

Gao, Y. G., Jiang, F. Y., Song, J. C., Zheng, L. J., Tian, F. Y., & Geng, P. L. (2018). A novel dual closed-loop control scheme based on repetitive control for grid-connected inverters with an LCL filter. *ISA Transactions*, *74*, 194–208. https://doi.org/10.1016/j.isatra.2018.01.029

Golzari, S., Rashidi, F., & Farahani, H. F. (2019). A Lyapunov function based model predictive control for three phase grid connected photovoltaic converters. *Solar Energy*, *181*(July 2018), 222–233. https://doi.org/10.1016/j.solener.2019.02.005

Hannan, M. A., Ghani, Z. A., Mohamed, A., & Uddin, M. N. (2014). Real-time testing of a fuzzy logic controller based grid-connected photovoltaic inverter system. *2014 IEEE Industry Application Society Annual Meeting, IAS 2014*, 1–8. https://doi.org/10.1109/IAS.2014.6978394

Huang, T., Shi, X., Sun, Y., & Wang, D. (2013). Three-phase Photovoltaic Grid-connected Inverter Based on Feedforward Decoupling Control. *2013 International Conference on Materials for Renewable Energy and Environment*, 476–480. https://doi.org/doi: 10.1109/ICMREE.2013.6893714.

Huerta, F., Pizarro, D., Cóbreces, S., Rodríguez, F. J., Girón, C., & Rodríguez, A. (2012). LQG servo controller for the current control of LCL grid-connected Voltage-Source Converters. *IEEE Transactions on Industrial Electronics*, *59*(11), 4272–4284. https://doi.org/10.1109/TIE.2011.2179273

Justin Boitano, J. B. . (n.d.). Advantages and Disadvantages of Controller Designs Using Fuzzy Logic. *Department of Computer Science and Engineering*. https://doi.org/https://citeseerx.ist.psu.edu/viewdoc/download?doi=10.1.1.36.8194&rep=rep1&type=pdf

Kalla, U. K. (2017). A normalized neural network based controller for power quality improved grid connected solar PV systems. *2016 IEEE 7th Power India International Conference, PIICON 2016*. https://doi.org/10.1109/POWERI.2016.8077467

Kaushik, H., Kalla, U. K., & Singh, B. (2020). Modified neural network algorithm-based control scheme of grid connected solar photovoltaic systems. *International Transactions on Electrical Energy Systems*, e12547. https://doi.org/10.1002/2050-7038.12547

Lalouni, S., & Rekioua, D. (2013). Optimal control of a grid connected photovoltaic system with constant switching frequency. *Energy Procedia*, *36*, 189–199. https://doi.org/10.1016/j.egypro.2013.07.022

Liang, X. (2017). Emerging Power Quality Challenges Due to Integration of Renewable Energy Sources. *IEEE Transactions on Industry Applications*, *53*(2), 855–866. https://doi.org/10.1109/TIA.2016.2626253

Liu, Z., Liu, J., & Zhao, Y. (2014). A unified control strategy for three-phase inverter in distributed generation. *IEEE Transactions on Power Electronics*, *29*(3), 1176–1191. https://doi.org/10.1109/TPEL.2013.2262078

Long, B., Cao, T., Fang, W., Chong, K. T., & Guerrero, J. M. (2021). Model Predictive Control of a Three-Phase Two-Level Four-Leg Grid-Connected Converter Based on Sphere Decoding Method. *IEEE Transactions on Power Electronics*, *36*(2), 2283–2297. https://doi.org/10.1109/TPEL.2020.3006432

M. vinary Kumar, U. salama. (2020). Modeling and simulation of a three phase grid connected photovoltaic system. *European Journal of Molecular & Clinical Medicine*, *7*(5), 244–261. https://doi.org/10.37082/ijirmps.2020.v08i06.010

Mohamed Rida, B., Rahli, M., Slami, S., & Hassaine, L. (2018). PSO based Direct Power Control for a Multifunctional Grid Connected Photovoltaic System. *International Journal of Power Electronics and Drive Systems (IJPEDS)*, *9*(2), 610. https://doi.org/10.11591/ijpeds.v9.i2.pp610-621

Mosazadeh, S. Y., Fathi, S. H., Hajizadeh, M., & Sheykholeslami, A. R. (2012). Adaptive hysteresis band controlled grid connected PV system with active filter function. *2012 International Conference on Power Engineering and Renewable Energy, ICPERE 2012*, *July*, 5–10. https://doi.org/10.1109/ICPERE.2012.6287253

Obi, M., & Bass, R. (2016). Trends and challenges of grid-connected photovoltaic systems - A review. *Renewable and Sustainable Energy Reviews*, *58*, 1082–1094. https://doi.org/10.1016/j.rser.2015.12.289

Pandiarajan, N., Ramaprabha, R., & Muthu, R. (2012). Application of circuit model for photovoltaic energy conversion system. *International Journal of Photoenergy*, *2012*. https://doi.org/10.1155/2012/410401

Patil, D. G. P. V. P. (n.d.). POWER QUALITY ISSUES IN GRID CONNECTED PHOTOVOLTAIC SYSTEM | International Engineering Journal For Research & Development. Retrieved July 28, 2021, from http://iejrd.com/index.php/ /article/view/1770

Patsalides, M., Evagorou, D., Makrides, G., Achillides, Z., Georghiou, G. E., Stavrou, A., Efthimiou, V., Zinsser, B., Schmitt, W., & Werner, J. H. (2007). The effect of solar irradiance on the power quality behaviour of grid connected photovoltaic systems. *Renewable Energy and Power Quality Journal*, *1*(5), 323–330. https://doi.org/10.24084/repqj05.284

Rahim, N. A., Selvaraj, J., & Krismadinata. (2007). Hysteresis current control and sensorless MPPT for grid-connected photovoltaic systems. *IEEE International Symposium on Industrial Electronics*, 572–577. https://doi.org/10.1109/ISIE.2007.4374659

Ramalingeswara Rao, K., & Srikanth, K. S. (2014). Improvement of power quality using fuzzy logic controller in grid connected photovoltaic cell using UPQC. *International Journal of Power Electronics and Drive Systems*, *5*(1), 101–111. https://doi.org/10.11591/ijpeds.v5i1.6184

Reveles-Miranda, M., Flota-Banuelos, M., Chan-Puc, F., Ramirez-Rivera, V., & Pacheco-Catalan, D. (2020). A Hybrid control technique for harmonic elimination, power factor correction, and night operation of a grid-connected pv inverter. *IEEE Journal of Photovoltaics*, *10*(2), 664–675. https://doi.org/10.1109/JPHOTOV.2019.2961600

Sathiyanarayanan, T., & Mishra, S. (2016). Synchronous reference frame theory based model predictive control for grid connected photovoltaic systems. *IFAC-PapersOnLine*, *49*(1), 766–771. https://doi.org/10.1016/j.ifacol.2016.03.149

Selvaraj, J., & Rahim, N. A. (2009). Multilevel Inverter For Grid-Connected PV System Employing Digital PI Controller. *IEEE Transactions on Industrial Electronics*, *56*(1), 149–158. https://doi.org/10.1109/TIE.2008.928116

Sinha, A., Chandra Jana, K., & Kumar Das, M. (2018). An inclusive review on different multi-level inverter topologies, their modulation and control strategies for a grid connected photo-voltaic system. *Solar Energy*, *170*(April), 633–657. https://doi.org/10.1016/j.solener.2018.06.001

Tariq, M., Iqba, M. T., Merap, M., Iqbal, A., Maswood, A. I., & Bharatiraja, C. (2017). Design of a proportional resonant controller for packed U cell 5 level inverter for grid-connected applications. *IEEE International Conference on Power Electronics, Drives and Energy Systems, PEDES 2016*, *2016-Janua*, 1–6. https://doi.org/10.1109/PEDES.2016.7914543

Villalva, M. G., Gazoli, J. R., & Ruppert Filho, E. (2009). Modeling and circuit-based simulation of photovoltaic arrays. *2009 Brazilian Power Electronics Conference, COBEP2009*, 1244–1254. https://doi.org/10.1109/COBEP.2009.5347680

Xie, B., Mao, M., Zhou, L., Wan, Y., & Hao, G. (2020). Systematic design of linear quadratic regulator for digitally controlled grid-connected inverters. *IET Power Electronics*, *13*(3), 557–567. https://doi.org/10.1049/IET-PEL.2019.0514

Ye, T., Dai, N., Lam, C., Wong, M., & Guerrero, J. M. (2016). Analysis , Design and Implementation of a Quasi-Proportional-Resonant Controller for a Multi- Functional Capacitive-Coupling Grid-Connected Inverter.

Zeb, K., Uddin, W., Khan, M. A., Ali, Z., Ali, M. U., Christofides, N., & Kim, H. J. (2018). A comprehensive review on inverter topologies and control strategies for grid connected photovoltaic system. *Renewable and Sustainable Energy Reviews*, *94*(June), 1120–1141. https://doi.org/10.1016/j.rser.2018.06.053

Zhu, Y., & Fei, J. (2017). Adaptive Global Fast Terminal Sliding Mode Control of Grid-connected Photovoltaic System Using Fuzzy Neural Network Approach. *IEEE Access*, *5*, 9476–9484. https://doi.org/10.1109/ACCESS.2017.2707668